

Cool Customers in the Stellar Graveyard I: Limits to Extrasolar Planets around the White Dwarf G29-38

John H. Debes¹, Steinn Sigurdsson¹, Bruce E. Woodgate²

ABSTRACT

We present high contrast images of the hydrogen white dwarf G 29-38 taken in the near infrared with the Hubble Space Telescope and the Gemini North Telescope as part of a high contrast imaging search for substellar objects in orbit around nearby white dwarfs. We review the current limits on planetary companions for G29-38, the only nearby white dwarf with an infrared excess due to a dust disk. We add our recent observations to these limits to produce extremely tight constraints on the types of possible companions that could be present. No objects $> 6 M_{Jup}$ are detected in our data at projected separations > 12 AU, and no objects $> 16 M_{Jup}$ are detected for separations from 3 to 12 AU, assuming a total system age of 1 Gyr. Limits for companions at separations < 3 AU come from a combination of 2MASS photometry and previous studies of G29-38's pulsations. Our imaging with Gemini cannot confirm a tentative claim for the presence of a low mass brown dwarf. These observations demonstrate that a careful combination of several techniques can probe nearby white dwarfs for large planets and low mass brown dwarfs.

Subject headings: circumstellar matter — planetary systems — white dwarfs — stars: individual (G29-38)

1. Introduction

G29-38 (ZZ Psc, WD 2326+049, GJ 895.2) is a nearby ($d=13.6$ pc) non-radially pulsating hydrogen white dwarf (WD) with photospheric absorption lines due to metals such as Mg and Ca (van Altena et al. 2001; Koester et al. 1997). Hydrogen WDs with metal absorption lines are known as DAZs. G29-38 has a measured gravity $\log g= 8.15$ and a $T_{eff}=11820$ K, placing its cooling age at 0.6 Gyr (Liebert et al. 2005).

¹Department of Astronomy & Astrophysics, Pennsylvania State University, University Park, PA 16802

²NASA Goddard Space Flight Center, Greenbelt, MD 27710

G29-38 possesses an infrared excess, originally attributed to a companion substellar object (Zuckerman & Becklin 1987). Further infrared studies, including pulsational studies in the near-IR, showed that the excess was more consistent with a circumstellar disk at $1 R_{\odot}$ with a blackbody temperature of ~ 1000 K (Tokunaga et al. 1988, 1990; Telesco et al. 1990; Graham et al. 1990). The origin of the disk is unclear, though it could be caused by a tidally disrupted asteroid or comet, potentially sent to the inner system by a planetary system that suffered chaotic evolution after post main sequence evolution (Debes & Sigurdsson 2002; Jura 2003).

Long-term pulsational studies of G29-38 have allowed several of the more stable pulsation modes to be monitored for timing delays due to an unseen companion (Kleinman et al. 1994, 1998). No conclusive detection of a companion has been reported. Speckle imaging of G29-38 furthermore could not detect any unresolved companions, although IR slit scans of G29-38 appeared to show an extension in the N-S direction on scales of $0.4''$ (Kuchner et al. 1998; Haas & Leinert 1990).

The biggest question that remains is the origin of the dust disk, which pollutes the white dwarf’s atmosphere with metals. Any origin for the dust requires a substellar companion (Debes & Sigurdsson 2002; Zuckerman et al. 2003). Planets in inner regions most likely are engulfed by the AGB phase of the star, with larger planets possibly “recycled” into brown dwarf companions (Siess & Livio 1999a,b). Remnant asteroids and comets potentially could survive at distances where they would not be ablated during the AGB phase (Stern et al. 1990). However, if the primary star has asymmetric mass loss, objects such as comets can easily be lost from the system if the orbital timescale equals the timescale for mass loss (Parriott & Alcock 1998). Planets or brown dwarfs in orbits $\gtrsim 5$ AU will avoid engulfment and survive post main sequence evolution (Rasio et al. 1996; Duncan & Lissauer 1998). Massive white dwarfs that are the result of WD-WD mergers may also form terrestrial mass planets in the debris of the merger, allowing unseen companions in close orbits (Livio et al. 1992).

WDs also make excellent targets for extrasolar planet searches with current ground and space based techniques (Burleigh et al. 2002; Debes et al. 2005). WDs are orders of magnitude dimmer than their main sequence progenitors, allowing fainter companions to be detected. In the near-IR substellar companions emit thermal radiation, which for objects warmer than ~ 300 K dominates the reflected light from their hosts. Companions that form at a particular semi-major axis conserve angular momentum during post main sequence mass loss and widen their orbits by a factor $\propto m_i/m_f$, where m_i and m_f are the initial and final masses of the central star (Jeans 1924). Any observations of a WD then probe to orbits that were a factor of at least 2 times smaller when the star was on the main sequence. Current

imaging searches in the near infrared are most effective for WDs that have a combined cooling time and main sequence age of $\sim 1\text{-}5$ Gyr. At these ages WDs have become dimmer than their main sequence progenitor. Concurrently, massive planets and brown dwarfs are observable in the near-IR since they haven't cooled below 300 K. WDs with metal lines can be markers for planetary systems and the presence of a dust disk and a high abundance of accreted metals makes G29-38 a primary candidate for the presence of a substellar or planetary companion (Debes & Sigurdsson 2002).

These motivations are the basis for a survey of nearby young DAZs that we have conducted using the Hubble Space Telescope (HST). We have primarily used the coronagraph on the NIC2 detector which is part of NICMOS. With the high contrast, resolution, and sensitivity of NICMOS, we can probe to within 3 AU of G29-38 looking for substellar companions that could help to explain the presence of this peculiar DAZ's dust disk. Section 2 describes the observations. Section 3 presents sensitivity limits as well as second epoch data for a candidate companion. These results are then combined with pulsational timing studies and 2MASS photometry to perform the most comprehensive search for substellar companions around a WD to date, providing a roadmap for the direct detection of planetary companions to WDs in the future. In Section 4 we present the conclusions from our work.

2. Observations

We imaged G29-38 using the NIC-2 camera on NICMOS both with and without a coronagraph. We used both the F110W ($\sim J$) and F160W ($\sim H$) filters for our observations. The highest degree of contrast at separations $> 1''$ is gained by performing a combination of coronagraphy and point spread function (PSF) subtraction (Fraquelli et al. 2004). Pipeline reduced coronagraphic data were obtained from STScI, and the basic procedure outlined by Fraquelli et al. (2004) was used to optimize the results for coronagraphic self-subtraction.

Due to the detection of a candidate planetary companion, follow-up observations were taken approximately a year later with Gemini North telescope Director's Discretionary time. We used the Altair adaptive optics (AO) system in conjunction with NIRI to take H band images of G 29-38 and the candidate to determine if they shared common proper motion.

The Gemini observations were taken on August 5, 2004. A total of $4 \times 15\text{s}$ frames were co-added at 10 dither points to subtract the background and to remove pixel-to-pixel defects, for an effective integration on source of forty minutes. Our total integration returned an average AO corrected FWHM of 75 mas, significantly smaller than the diffraction limit of our F110W images with HST. Because of Gemini's higher spatial resolution, we used this

second epoch data to search for companions at separations $<1''$. Table 1 shows the date and time of the observations taken of G29-38, along with the filters.

The second epoch Gemini data were processed using several IRAF tasks designed by the Gemini Observatory and based upon the samples given to observers. Each frame was flatfielded and sky subtracted. In addition, due to the on-sky rotation from a fixed Cassegrain Rotator, each frame was rotationally registered and combined. More details of the general strategy and reduction are in Debes et al. (2005).

3. Results

No substellar objects were detected in an annulus between $1''$ and $5''$ from G 29-38 with our coronagraphic observations. One candidate object was detected at a $S/N \sim 6$ with $m_{F110W} - m_{F160W} = 1.1 \pm 0.3$ and apparent $m_{F110W} = 23.7 \pm 0.2$. The discovery image and its follow up Gemini image is shown in Figure 1. The magnitudes and colors were consistent with an object $< 10 M_{Jup}$ at 13.6 pc (Burrows et al. 2003). Its initial position relative to G 29-38 was $\Delta\alpha = 4.91'' \pm 0.01$ $\Delta\delta = 2.03'' \pm 0.01$ in our HST images. Since the measured proper motion of G29-38 is -411 ± 0.01 mas/yr in α and -263 ± 0.01 mas/yr in δ (Pauli et al. 2003), we predict an increase of 330 mas and 250 mas in R.A. and declination, respectively, between our two epoch observations due to parallactic motion and proper motion, leading to $\Delta\alpha = 5.24'' \pm 0.02$ and $\Delta\delta = 2.28 \pm 0.02$ for the non co-moving case. The position of the candidate in the second epoch Gemini data is $\Delta\alpha = 5.25'' \pm 0.01$ and $\Delta\delta = 2.30'' \pm 0.01$.

The candidate is a background object that does not share G29-38’s proper motion. The errors in the calculation come primarily from the uncertainty in G29-38’s proper motion and uncertainties in the measured centroids. However, the position of the background object is well within the errors and shows no hint of its own proper motion.

Our Gemini data were of high enough spatial resolution that we should have easily detected extended structure similar to what was reported in Haas & Leinert (1990). We see no such structure in any of our HST or Gemini observations. Any dust disk present around G29-38 must be confined to smaller than 75 mas or 1 AU projected separation.

3.1. Limits from Imaging

Schneider & Silverstone (2003) showed a reliable way to determine sensitivity of an observation with NICMOS, given the stability of the instrument. Artificial “companions”

are generated with the HST PSF simulation software TINYTIM¹ and scaled to higher fluxes until they are recovered. These companions are inserted into the observations and used to gauge sensitivity. We adopted this strategy for our data as well. An implant was placed in the images. Two difference images were created following our procedure of PSF subtraction and then rotated and combined for maximum signal to noise. Sample images were examined by eye as a second check that the dimmest implants could be recovered. The implants were normalized so that their total flux was equal to 1 DN/s. The normalized value was converted to a flux in Jy or a Vega magnitude by multiplying by the correct photometry constants given by the NICMOS Data Handbook. We considered an implant recovered if its scaled flux in a given aperture had a S/N of 5.

For our Gemini data we used the PSF of G29-38 as a reference for the implant. The implant was normalized to a peak pixel value of one. Implants were scaled with increasing flux until recovered to determine the final image’s sensitivity to objects at a S/N of 10, since significant flux from the PSF remained at separations $< 1''$. The relative flux of the implant with respect to the host star was measured and a corresponding MKO H magnitude was derived from the 2MASS H magnitude to give a final apparent magnitude sensitivity. For our Gemini images we checked sensitivity starting at a distance of ~ 3 times the FWHM of G29-38, or $0.22''$, out to $7''$, the extent of our field of view. Gemini’s sensitivity beyond $\sim 1.5''$ was comparable to that of our NICMOS data, with a median sensitivity of $H \sim 22.9$.

Our resulting sensitivity plot in Figure 2, incorporating both our Gemini and HST data, shows the apparent limiting magnitudes in our search from $0.22''$ to $5''$. These results represent the deepest and highest contrast images taken around a white dwarf to date. In the NICMOS images beyond $1''$ our sensitivity was limited not by scattered light from G 29-38, but by the limited exposure time.

It is useful to convert the sensitivity in the observed magnitudes or fluxes into a corresponding companion mass. Since most substellar companions do not have long term energy sources, the luminosity of a brown dwarf or planet that is not significantly insolated is dependent both on mass and age. In the present situation we can estimate the age of the system based on the properties of the host star. For our current sensitivity calculation we chose the most recent models published by Burrows et al. (2003) and Baraffe et al. (2003). These models are difficult to compare to each other and to observations in the near-IR due to the presence of H₂O molecular absorption that can cause variations in predicted magnitudes in different photometric systems (Stephens & Leggett 2004). The Baraffe et al. (2003) magnitudes are in the CIT system, while Burrows et al. (2003) make their synthetic spectra

¹<http://www.stsci.edu/software/tinytim/tinytim.html>

directly available and thus can be convolved with any filter set. Both sets converge to within a magnitude of each other for ages > 1 Gyr in the J, H, and K filters but in general, for a given age and mass, the Burrows et al. (2003) predicted magnitudes are fainter. In Figure 3 and our calculations in this Section, we use the Burrows et al. (2003) models. If the Baraffe et al. (2003) models are correct, our limits are at most $\sim 1-2 M_{Jup}$ lower than reported. In Section 3.2 we instead use the Baraffe et al. (2003) models since they extend to higher mass.

Most models are for ground based J, H, and K filters. These filters were originally designed to avoid atmospheric windows of high near-IR absorption which is irrelevant for HST filter design. The wideband NICMOS filters vaguely resemble their ground-based counterparts, but possess significant differences in the case of objects that have deep molecular absorption. To adequately understand what type of companions one can detect, it is necessary to take flux calculations from the models and convolve them with the waveband of interest to get a predicted absolute magnitude for the HST filters:

$$M_x = -2.5 \log \left(\int \lambda A_\lambda F_\lambda d\lambda \right) + 2.5 \log \left(\int \lambda A_\lambda F_{\lambda, Vega} d\lambda \right) \quad (1)$$

where A_λ is the transmission function of the filter, F_λ is the flux of the putative companion, and $F_{\lambda, Vega}$ is the Vega flux as calculated by Kurucz (1979). This method is preferred for detector arrays when calculating synthetic photometry (Girardi et al. 2002).

Figure 3 shows a sample M_{F110W} vs. $M_{F110W} - M_{F160W}$ color magnitude plot for substellar objects as a function of their mass that have ages of 1 Gyr and 3 Gyr (Burrows et al. 2003). A comparison with Burrows et al. (2003)'s plots show that the predicted J magnitudes in their paper and the F110W magnitudes we've calculated differ by slight amounts due to the different transmission function of the two filters. It should also be noted that these predicted fluxes are based upon a completely isolated object that is not experiencing any insolation from its host star. Companions around WDs would have been insolated by their parent star for the main sequence lifetime. However, insolation calculations show that this would be insignificant for well separated companions (Burrows et al. 2004). The largest insolation would occur during the red giant branch (RGB) and asymptotic giant branch phases (AGB) of post main sequence evolution. Calculating the equilibrium temperature shows that the temperature at 5 AU during these phases would be less than the temperature experienced by HD 209458B, the Jovian planet in a 0.03 AU orbit around a main sequence star. Insolation of a planet during the post main sequence stages of evolution should not be sufficient to alter a substellar companion's predicted magnitude from the isolated case.

To get a final prediction of the types of companions to which we are sensitive requires a fairly accurate estimate of the WDs total age. The total age can be determined from the sum of a WDs cooling age and its main sequence lifetime. Estimates of the main sequence

lifetime can be taken from the initial to final mass ratio relationship between WDs and their progenitor stars (Weidemann 2000). Cooling times can be derived by modeling. Liebert et al. (2005) gives G29-38’s mass and cooling age as $0.7 M_{\odot}$ and 0.6 Gyr. Using a theoretical version of the initial-to-final mass function, $M_i = 10.4 \ln [(M_{WD}/ M_{\odot})/0.49] M_{\odot}$, one derives an initial mass of $3.7 M_{\odot}$ (Wood 1992). The main sequence (MS) lifetime can be estimated by $10(M/M_{\odot})^{-2.5}$ Gyr, which gives an MS lifetime of 0.4 Gyr and thus a total age of 1 Gyr (Wood 1992). However, from pulsational studies, the precise mass of G 29-38 is $0.6 M_{\odot}$ which, if the cooling time remains the same or is a bit longer, leads to an age of 2-3 Gyr (Kleinman et al. 1998). Thus, the age of G 29-38 likely lies between 1 and 3 Gyr.

3.2. Limits from 2MASS Photometry

While direct imaging is most sensitive to companions $>0.2''$ unresolved companions could still be present for G29-38. In order to rule out companions at separations where imaging or PSF subtraction could not resolve them, we looked at the near-IR flux of G29-38. Low mass companions to WDs have often been discovered through near-IR excesses (Probst & Oconnell 1982; Zuckerman & Becklin 1992; Green et al. 2000). G29-38 presents a problem due to its already well known dust disk, which causes a measurable excess starting at about $1.6\mu\text{m}$. However, no large excess is predicted for the J band, which we will use to limit the presence of unresolved substellar companions. For our search we use the near-IR photometry of the 2MASS catalogue which has been used in the past to search for flux excesses in combination with comparison to model WD atmospheres (Wachter et al. 2003). Using the measured effective temperatures, gravities, and distances of a WD, we can model the expected J magnitude (J_{th}) using the model atmospheres of Bergeron et al. (1995). These models cover a wide range of WD effective temperature, gravity, and atmospheric composition. When combined with accurate photometry in the visible, these models can reproduce the flux in the J band of a WD to within a few percent (Bergeron et al. 2001). The model values of J, H, and K are based on the CIT filter system, which we converted to 2MASS magnitudes using the color transformations provided by the 2MASS documentation². Then, the excess of the expected minus observed J magnitude, $\Delta J = J_{th} - J_{2MASS}$, can be determined. An excess of flux in the J band under this notation gives a positive ΔJ . At the accuracy of 2MASS, limits can be placed on the type of companions present in close orbit around G29-38.

In order to place robust limits to a J excess for G29-38, we must determine the scatter

²http://www.ipac.caltech.edu/2mass/releases/allsky/doc/sec6_4b.html

of ΔJ from a sample of WDs with known physical parameters and see what an accurate estimate of a 3σ excess would be. We would expect the sample to have a median $\Delta J \sim 0$ and that the standard deviation of ΔJ gives a good estimate of the 1σ error in our analysis. As a demonstration we take the sample of Liebert et al. (2005) which includes G29-38 in a study of DA WDs from the PG survey of UV excess sources. Of the 374 white dwarfs we chose the brightest 72 of the sample that had a $J < 15$, had unambiguous sources in 2MASS, and had reliable photometry, i.e those objects that had quality flags of A or B in the 2MASS point source catalogue for their J magnitudes.

If there were a significant number of excesses in the sample then the standard deviation of the observed minus expected magnitudes will be overestimated. Since we cannot *a priori* know whether there will be a large number of excesses or not, we’ve assumed that there are not a significant fraction of WDs with excesses in our samples. While calculating the standard deviation for each filter, we removed any object with an excess $> 3\sigma$ from the sample and recalculated the scatter in observed minus expected magnitudes. We iterated this process three times. We found that of the 72 sources, only eight objects showed an excess in at least one filter. These objects are in Table 2.

After determining the standard deviation of the sample, we found that 1σ errors for the sample in the J, H, and K bands were 0.07 mag, 0.1 mag, and 0.15 mag, respectively. We treated any excesses greater than 3σ as significant, though if an excess was only present in one band we marked this as a tentative detection. One exception is G29-38 itself, which showed only a 3.5σ excess in the Ks band due to its dust disk, which has been amply confirmed in the past.

Seven objects in our sample showed significant excesses in at least two filters and one object showed a significant excess only in the Ks band. These results are shown in Table 2. Of the eight objects, 5 were previously known (See references in Table 2). PG 1234+482, PG 1335+369, and PG 1658+441 are new. Care was taken to ensure that the coordinates of new excess candidates in the 2MASS fields were correct and that their optical photometry was consistent both with that reported in Liebert et al. (2005) and with the distance assumed in the modeling. The absolute magnitudes of candidate excess companions were calculated by taking the excess flux and using the distance derived from models of the WDs. A spectral type for each excess object was either taken from the literature or compared to nearby M and L dwarfs with known distances (Henry et al. 1994; Leggett et al. 2001). The results are presented in Table 3. The spectral types we’ve determined are rough and need to be confirmed through spectroscopic follow-up or high spatial resolution imaging.

PG 1234+482 and PG 1658+441 both were previously studied in the J and K bands by Green et al. (2000) for excesses. None were reported for either of these objects. Based on our

analysis, PG 1234+482 has significant excesses in the H and Ks filters. Green et al. (2000) reported a similar K magnitude as that reported in 2MASS but due to larger errors in their photometry, measured it as a marginal excess of $\sim 1.3\sigma$. PG 1658+441 shows only an excess in the Ks 2MASS filter, which is contradicted by the infrared photometry taken in Green et al. (2000). Their measured magnitude in K differs by ~ 0.6 mag from 2MASS, with the 2MASS measurements having a higher reported error. Based on this uncertain photometry, the excess could be due to a mid L dwarf—the J-K color of such an object would result in a negligible excess in J and an observable excess in K_s (Leggett et al. 2001). This would be an exciting discovery, if confirmed, as only two substellar objects are known to orbit nearby white dwarfs (Becklin & Zuckerman 1988; Farihi & Christopher 2004) PG 1658+441 has been selected and observed for Program 10255, an HST snapshot program to resolve close WD+M dwarf binaries. If an L dwarf is present in an orbit greater than a few AU, it should be resolved with those observations.

Our resulting 3σ limit for G29-38 is then $\Delta J=0.21$, which corresponds to an unresolved source with $M_J=14.8$. Interpolating from the models of (Baraffe et al. 2003), the corresponding unresolved companion mass at 1 and 3 Gyr is $40 M_{Jup}$ and $58 M_{Jup}$ respectively.

3.3. Limits from Pulsational Studies

Claims for the presence of companions around G29-38 have often occurred. Its infrared excess was originally attributed to a brown dwarf companion, while radial velocity and pulsational timing hinted at the presence of either a low mass stellar companion or a massive black hole, all of which were shown to be spurious by more careful, long-term pulsational timing (Kleinman et al. 1994).

Pulsational timing is done in a similar fashion to pulsar timing, in that phase changes of the observed minus calculated (O-C) pulse arrival times can be used to calculate the projected semi-major axis of the reflex motion for the white dwarf, $a \sin i$. For pulsating white dwarfs, the technique requires identifying a stable pulsational mode and measuring its arrival time very precisely. Measuring higher derivatives of the period change can also help to further constrain the Keplerian parameters of a companion orbit before it has completed a full revolution. This technique for pulsars has been remarkably effective at finding “oddball” planets, such as the first terrestrial extrasolar planets ever discovered and a Jovian mass planet in the metal poor M4 cluster (Wolszczan & Frail 1992; Sigurdsson et al. 2003).

Long baseline timing studies of pulsating white dwarfs can produce very stringent limits to the types of companions orbiting them, down to tens of Earth masses. They are limited by

the timescale of observations and knowledge of the inclination of the system while probing the inner-most orbital separations. In this sense pulsational timing is generally complementary to direct imaging searches, the combination of the two providing a comprehensive and sensitive method for searching for extra-solar planets.

Kleinman et al. (1994) demonstrated that for G29-38, perturbations on the order of 10 s or greater could have been detected around the white dwarf. In fact, a trend was discovered in their data that had an amplitude of 56 s and a possible period of 8 years. This was a tentative detection given the possibility of the mode that they used being unstable or slowly varying. However, based on G29-38’s parameters, one can estimate how massive such a companion would be and what its semi-major axis would be assuming $i \sim 90^\circ$. Assuming G29-38 has a mass of $0.6 M_\odot$, the derived minimum mass was $21 M_{Jup}$ with a semi-major axis of 3.4 AU. A mass of $0.7 M_\odot$ does not significantly change these values.

As mentioned above, the noise limit to the Kleinman et al. (1994) pulsational timing allows limits to be placed on the types of companions present with orbital timescales of < 8 years. Figure 4 shows the combination of the pulsational timing limits based on the 10 s noise limit and our observational data. Our 2MASS photometry limits extend to where the predicted mass equals that derived from the limits of the pulsational studies, 0.4 AU for an age of 1 Gyr and 0.2 AU for an age of 3 Gyr. Between those separations and 3 AU, the limits are determined by the pulsational studies. Beyond 3 AU the limits are determined by our imaging. Overplotted is the separation and mass of the possible companion detected in the pulsational timing. Our observations weigh against the possibility of the tentative companion, if the total age of G29-38 is closer to 1 Gyr. If the age of G29-38 is closer to 3 Gyr, we can constrain the inclination of the possible companion’s orbit to be $> 44^\circ$ from face on based on our detection limit of $30 M_{Jup}$. Inspection of the limits shows that any companion $> 12 M_{Jup}$ is ruled out for separations between ~ 1 AU and 3 AU and > 5 AU if the age of G 29-38 is close to 1 Gyr. All but planetary mass objects are ruled out for a good portion of the discovery space around this white dwarf. Further observations, such as sensitive radial velocity variations, would provide a stronger limit to close in companions than what is possible with 2MASS.

4. Conclusions

We have shown that a combination of high contrast imaging and photometry of individual relatively young and nearby white dwarfs such as G 29-38 can effectively probe for high mass planets. Information gleaned through this technique we can detect planets not accessible by other methods. Any planet discovered could become an important spectroscopic

target for follow-up. The information gleaned from a large scale version of this study may provide key information on planet formation and evolution in intermediate mass stars as well as providing a possible explanation for the origin of white dwarfs with metal absorption (Debes & Sigurdsson 2002).

If a close companion is involved in the origin of G29-38’s dusty disk, it must be substellar and if a well-separated companion is involved it is of planetary mass. These mass limits apply if the scenario for the formation of DAZs follows Debes & Sigurdsson (2002), where an unstable planetary system sends volatile-depleted asteroidal or cometary material into the inner system. The possibility remains that a smaller planet could be present. Indeed, planets of $\sim 1 M_{Jup}$ or less may be favored for the DAZ phenomenon (Hansen 2004, private communication). Planets near our mass limits may be too efficient at ejecting surviving planetesimals rather than sending them into the inner system.

Finally, due to the sensitivity of our Gemini observations we can place some strong conclusions on previous claims for the presence of close companions due to pulsational timing by Kleinman et al. (1994). If the age of G29-38 is 1 Gyr, we can refute the presence of a companion at ~ 3.4 AU. We can place limits on its mass if the age of G29-38 is closer to 3 Gyr. The possibility exists that the companion could be closer to G 29-38 than its maximum extent, since the pulsation timing observations were of not sufficient quality to determine the phase of the initial observations. We see no evidence for a companion beyond some structure in the AO PSF at a projected separation that does not match the predicted orbital separation (Trujillo 2004, personal communication).

We would like to gratefully acknowledge Al Shultz and Glenn Schneider for helpful conversations about coronagraphy with NICMOS, and Chad Trujillo and Joe Jensen for critical help with the inner workings of Altair and the reduction of Altair imaging data.

Based on observations made with the NASA/ESA Hubble Space Telescope, obtained at the Space Telescope Science Institute, which is operated by the Association of Universities for Research in Astronomy, Inc., under NASA contract NAS5-26555. These observations are associated with program #9834. Also based on observations obtained at the Gemini Observatory, which is operated by the Association of Universities for Research in Astronomy, Inc., under a cooperative agreement with the NSF on behalf of the Gemini partnership: the National Science Foundation (United States), the Particle Physics and Astronomy Research Council (United Kingdom), the National Research Council (Canada), CONICYT (Chile), the Australian Research Council (Australia), CNPq (Brazil) and CONICET (Argentina). Near-IR Photometry obtained as part of the Two Micron All Sky Survey (2MASS), a joint project of the University of Massachusetts and the Infrared Processing and Analysis

Center/California Institute of Technology, funded by the National Aeronautics and Space Administration and the National Science Foundation. S.S. also acknowledges funding under the Pennsylvania State University Astrobiology Research Consortium (PSARC).

REFERENCES

- Allard, F., Wesemael, F., Fontaine, G., Bergeron, P., & Lamontagne, R. 1994, *AJ*, 107, 1565
- Baraffe, I., Chabrier, G., Barman, T. S., Allard, F., & Hauschildt, P. H. 2003, *A&A*, 402, 701
- Becklin, E. E. & Zuckerman, B. 1988, *Nature*, 336, 656
- Bergeron, P., Leggett, S. K., & Ruiz, M. T. 2001, *ApJS*, 133, 413
- Bergeron, P., Wesemael, F., Lamontagne, R., Fontaine, G., Saffer, R. A., & Allard, N. F. 1995, *ApJ*, 449, 258
- Burleigh, M. R., Clarke, F. J., & Hodgkin, S. T. 2002, *MNRAS*, 331, L41
- Burrows, A., Sudarsky, D., & Hubeny, I. 2004, *ApJ*, 609, 407
- Burrows, A., Sudarsky, D., & Lunine, J. I. 2003, *ApJ*, 596, 587
- Debes, J. H. & Sigurdsson, S. 2002, *ApJ*, 572, 556
- Debes, J. H., Sigurdsson, S., & Woodgate, B. 2005, (in preparation)
- Duncan, M. J. & Lissauer, J. J. 1998, *Icarus*, 134, 303
- Farihi, J. & Christopher, M. 2004, *AJ*, 128, 1868
- Fraquelli, D. A., Schultz, A. B., Bushouse, H., Hart, H. M., & Vener, P. 2004, *PASP*, 116, 55
- Girardi, L., Bertelli, G., Bressan, A., Chiosi, C., Groenewegen, M. A. T., Marigo, P., Salasnich, B., & Weiss, A. 2002, *A&A*, 391, 195
- Graham, J. R., Matthews, K., Neugebauer, G., & Soifer, B. T. 1990, *ApJ*, 357, 216
- Green, P. J., Ali, B., & Napiwotzki, R. 2000, *ApJ*, 540, 992
- Haas, M. & Leinert, C. 1990, *A&A*, 230, 87

- Hansen, B. 2004, Personal Communication
- Henry, T. J., Kirkpatrick, J. D., & Simons, D. A. 1994, *AJ*, 108, 1437
- Jeans, J. H. 1924, *MNRAS*, 85, 2
- Jura, M. 2003, *ApJ*, 584, L91
- Kleinman, S. J., et al. 1994, *ApJ*, 436, 875
- Kleinman, S. J., et al. 1998, *ApJ*, 495, 424
- Koester, D., Provencal, J., & Shipman, H. L. 1997, *A&A*, 320, L57
- Kuchner, M. J., Koresko, C. D., & Brown, M. E. 1998, *ApJ*, 508, L81
- Kurucz, R. L. 1979, *ApJS*, 40, 1
- Leggett, S. K., Allard, F., Geballe, T. R., Hauschildt, P. H., & Schweitzer, A. 2001, *ApJ*, 548, 908
- Liebert, J., Bergeron, P., & Holberg, J. B. 2005, *ApJS*, 156, 47
- Livio, M., Pringle, J. E., & Saffer, R. A. 1992, *MNRAS*, 257, 15P
- Parriott, J. & Alcock, C. 1998, *ApJ*, 501, 357
- Pauli, E.-M., Napiwotzki, R., Altmann, M., Heber, U., Odenkirchen, M., & Kerber, F. 2003, *A&A*, 400, 877
- Probst, R. G. & Oconnell, R. W. 1982, *ApJ*, 252, L69
- Rasio, F. A., Tout, C. A., Lubow, S. H., & Livio, M. 1996, *ApJ*, 470, 1187
- Schneider, G. & Silverstone, M. D. 2003, in *High-Contrast Imaging for Exo-Planet Detection*. Edited by Alfred B. Schultz. *Proceedings of the SPIE*, Volume 4860, pp. 1-9 (2003)., 1-9
- Siess, L. & Livio, M. 1999a, *MNRAS*, 304, 925
- . 1999b, *MNRAS*, 308, 1133
- Sigurdsson, S., Richer, H. B., Hansen, B. M., Stairs, I. H., & Thorsett, S. E. 2003, *Science*, 301, 193
- Stephens, D. C. & Leggett, S. K. 2004, *PASP*, 116, 9

- Stern, S. A., Shull, J. M., & Brandt, J. C. 1990, *Nature*, 345, 305
- Telesco, C. M., Joy, M., & Sisk, C. 1990, *ApJ*, 358, L17
- Tokunaga, A. T., Becklin, E. E., & Zuckerman, B. 1990, *ApJ*, 358, L21
- Tokunaga, A. T., Hodapp, K.-W., Becklin, E. E., Cruikshank, D. P., Rigler, M., Toomey, D., Brown, R. H., & Zuckerman, B. 1988, *ApJ*, 332, L71
- Trujillo, C. 2004, Personal communication
- van Altena, W. F., Lee, J. T., & Hoffleit, E. D. 2001, *VizieR Online Data Catalog*, 1238, 0
- Wachter, S., Hoard, D. W., Hansen, K. H., Wilcox, R. E., Taylor, H. M., & Finkelstein, S. L. 2003, *ApJ*, 586, 1356
- Weidemann, V. 2000, *A&A*, 363, 647
- Wolszczan, A. & Frail, D. A. 1992, *Nature*, 355, 145
- Wood, M. A. 1992, *ApJ*, 386, 539
- Zuckerman, B. & Becklin, E. E. 1987, *Nature*, 330, 138
- . 1992, *ApJ*, 386, 260
- Zuckerman, B., Koester, D., Reid, I. N., & Hünsch, M. 2003, *ApJ*, 596, 477

Table 1. Table of the observations taken of G29-38

Observation name	Date & Time(UT)	Filter	Exposure Time(s)
N8Q301010	2003-10-20 10:07:00	F205W	17.942
N8Q301011	2003-10-20 10:08:00	F205W	17.942
N8Q301020	2003-10-20 10:15:20	F160W	11.960
N8Q301030	2003-10-20 10:20:00	F110W	11.960
N8Q304010	2003-09-14 19:31:00	F110W	575.877
N8Q305010	2003-09-14 19:59:00	F110W	575.877
N8Q306010	2003-09-14 21:07:00	F160W	575.877
N8Q307010	2003-09-13 21:35:00	F160W	575.877
GN-2004A-DD-9	2004-08-05 14:81:08	MKO H	2220.00

Table 2. 2MASS Photometry of PG WDs

PG	J_{th}	H_{th}	$K_{s(th)}$	J	H	K_s
0017+061	15.33	15.49	15.56	13.74	13.19	12.98
0205+134	15.45	15.63	15.72	12.80	12.20	11.96
0824+289	14.95	15.13	15.22	12.42	11.80	11.65
1026+002	14.29	14.41	14.46	11.75	11.22	10.94
1033+464	14.93	15.08	15.17	12.56	12.03	11.75
1234+482	15.14	15.32	15.40	14.98	14.96	14.94
1335+369	15.03	15.15	15.20	13.29	12.92	12.85
1658+441	15.26	15.40	15.50	15.44	15.53	15.05

Table 3. Magnitudes and Spectral Types of Excess Candidates

PG	M_J	M_H	M_{K_s}	Sp Type	Reference
0017+061	8.98	8.29	8.05	M5V	1 ^a
0205+134	6.46	5.81	5.56	M3.5V	2
0824+289	6.90	6.24	6.09	dC+M3V	3
1026+002	8.96	8.38	8.09	M5V	1
1033+464	8.15	7.56	7.26	M4V	1
1234+482	11.31	10.3	10.3	M8V	- ^b
1335+369	9.30	8.84	8.77	M5.5V	- ^b
1658+441	-	-	14.1	L5	- ^b

References. — (1) Zuckerman & Becklin (1992) (2) Allard et al. (1994) (3) Green et al. (2000)

^aZuckerman & Becklin (1992) did not estimate spectral type, estimates taken from 2MASS magnitudes of nearby M dwarfs listed in Henry et al. (1994)

^bThis work used 2MASS magnitudes of nearby M dwarfs from Henry et al. (1994) and nearby L, T dwarfs from Leggett et al. (2001) to determine rough spectral types

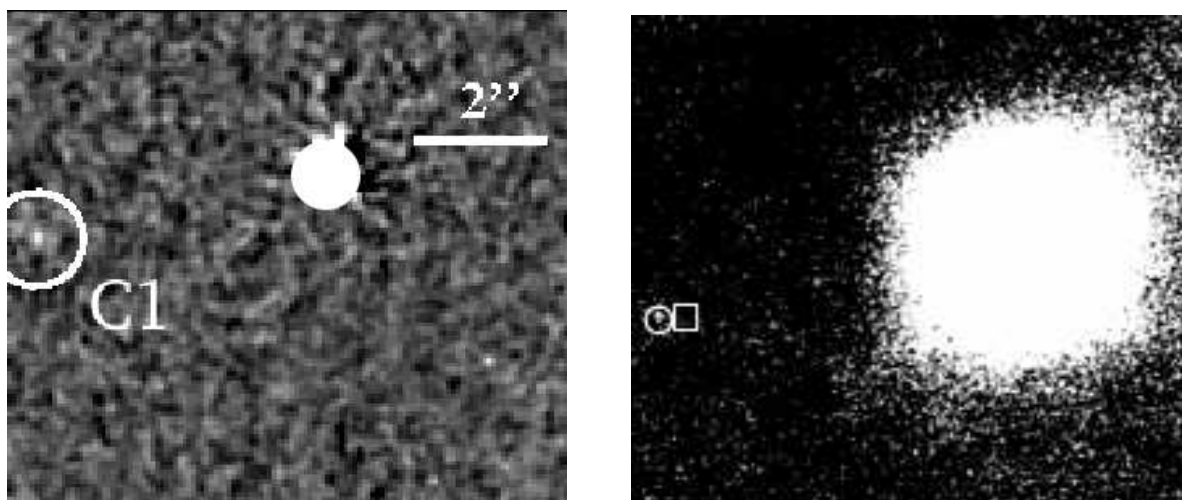


Fig. 1.— (left) Discovery image of a candidate planetary companion in the HST F160W filter. The image was smoothed with a Gaussian filter, C1 marks the candidate, and G29-38 is masked out. Other features are either subtraction artifacts or detector artifacts. (right) Second epoch image with Gemini, along with the predicted positions of co-moving (square) and non co-moving (circle) objects. The object is non co-moving and therefore in the background. In both images North is rotated 36° clockwise.

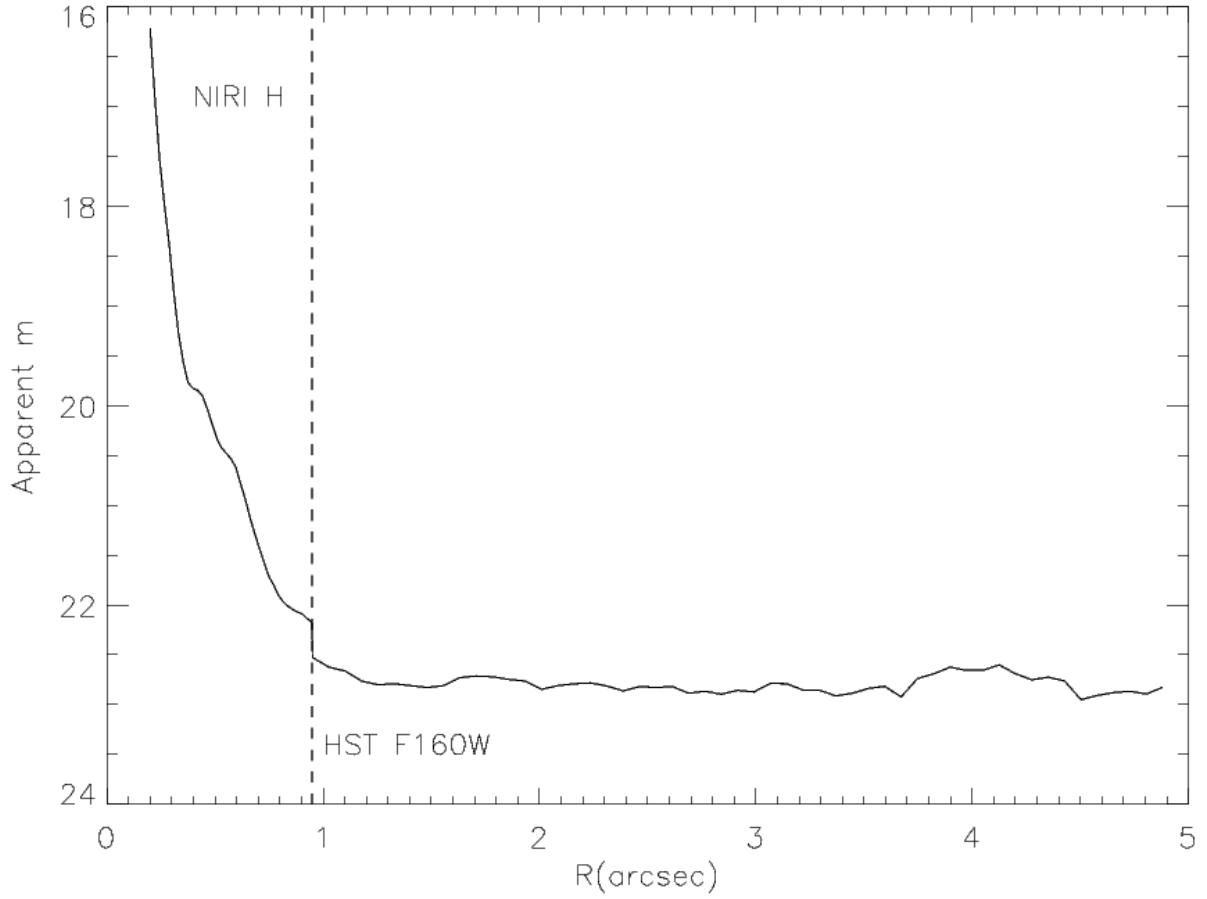


Fig. 2.— The final azimuthally averaged limiting magnitude curve of our HST and Gemini images. Our HST observations were sensitive to objects that had a S/N of > 5 at separations $> 1''$. At separations $< 1''$, The Gemini PSF still had significant flux. To ensure that our sensitivity reflected actual detectability, we used a S/N limit of $10 < 1''$.

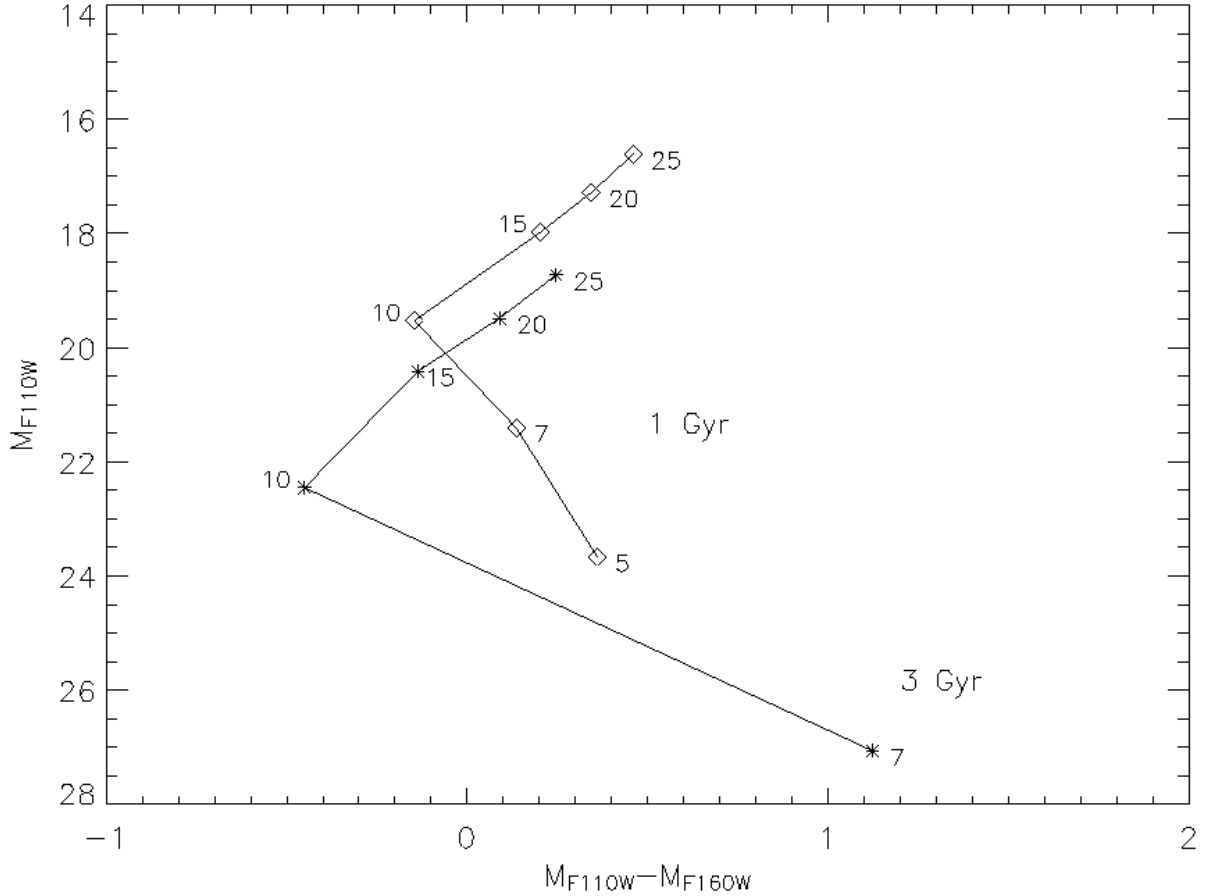


Fig. 3.— Color-magnitude diagram with isochrones of substellar objects with a total age of between 1 and 3 Gyr in NICMOS filters. We used the spectral models of Burrows et al. (2003) and convolved them with the NICMOS filters. Numbers on the isochrones refer to the mass in Jupiter masses. Numbers 10-25 follow the observed properties of T dwarfs and have bluer colors. At effective temperatures of < 400 K, water absorption suppresses flux in the F110W filter and again makes these objects redder. Colors are sensitive to this absorption and are uncertain.

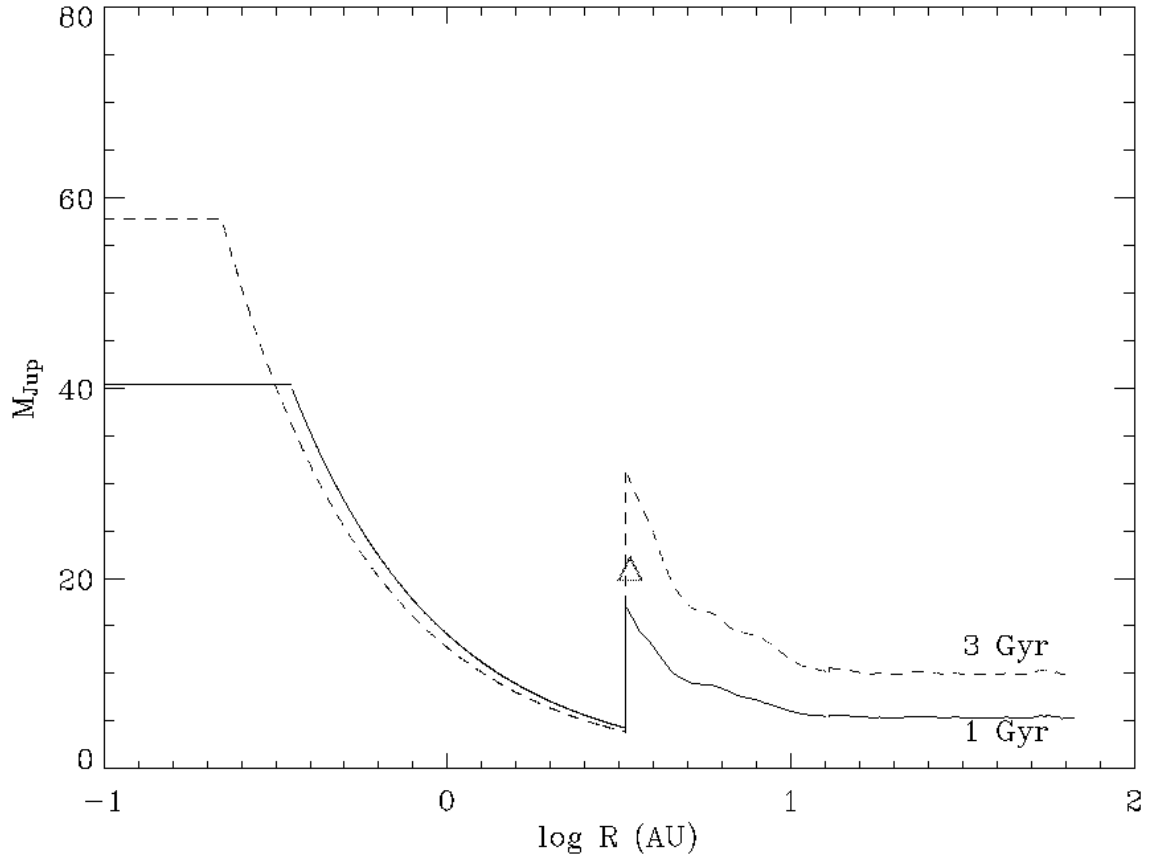


Fig. 4.— Combined limits to substellar objects around G29-38 from a combination of 2MASS photometry, pulsation studies, and our high contrast imaging. The solid and dashed lines show the limits for assumed total ages of 1 and 3 Gyr, respectively, and the triangle shows the expected minimum mass of a companion tentatively discovered by pulsational studies.